

Investigation of the Electrical Resistance of Single-Walled Carbon Nanotube Films in the Temperature Range 4.2–290 K

A. S. Lobach^a, L. I. Buravov^a, N. G. Spitsyna^a, A. V. Eletskii^b, A. P. Dementjev^b, and K. I. Maslakov^b

^a Institute of Problems of Chemical Physics, Russian Academy of Sciences,
pr. Akademika Semenova 1, Chernogolovka, Moscow Region, 142432, Russia

e-mail: lobach@icp.ac.ru

^b National Research Centre “Kurchatov Institute”, pl. Kurchatova 1, Moscow, 123182, Russia

Received November 8, 2010

Abstract—Electrical resistance of films made of the source material and purified HiPCO and Arc single-walled carbon nanotubes (SWCNTs) with a thickness of 20–40 μm is 2.4 to 45 Ω (electrical conductivity of 0.42×10^3 to $5.03 \times 10^3 \text{ S/m}$) at room temperature. The films have been formed by vacuum microfiltration of SWCNT suspensions in toluene and characterized by Raman and X-ray photoelectron spectroscopy and scanning electron microscopy. The conductivity of the films at room temperature depends on the type and degree of purity of the material of nanotubes. The resistance of the films decreases with the increasing temperature over the range of 4.2–290 K, and the rate of the step-down decreases with increasing purity of the material of the nanotubes. The conductivity of the films is semiconducting in character, and the electron transport is consistent with three-dimensional hopping conductivity.

DOI: 10.1134/S0018143911040102

Films based on single-walled carbon nanotubes, which feature an appropriate combination of electrical, optical and mechanical properties and high thermal and chemical stability, are of practical interest. SWCNT films have good electron transport properties and can be successfully integrated in organic photovoltaic devices as an electron-acceptor material in the solar cells of bulk-heterojunction type, as well as transparent electrodes replacing inorganic ITO ($\text{In}_2\text{O}_3 : \text{SnO}_2$) oxides [1, 2]. A high sensitivity of the electronic properties of carbon nanotubes (NTs) to the presence of attached chemical groups or adsorbed molecules on their surface opens a possibility to develop NT-based subminiature sensors [3, 4].

The electrical parameters of SWCNTs show a significant spread of values, which is caused by a variety of their structural features associated with a difference in the methods and conditions of their synthesis and purification. The major charge carriers determining the conductivity of NTs are electrons. In defect-free SWCNTs at low temperatures the electrons move along the NTs without scattering, which corresponds to the quantum ballistic conduction mechanism. The data on the electric resistance of SWCNTs at room temperature have a significant spread of values (in the range from 1.5 to $10^4 \text{ k}\Omega$ for individual NTs, from 1.5 to $14 \text{ k}\Omega$ for NT bundles, and from 3 to 12Ω for fabric material of NTs [5]). This spread indicates the dependence of the electrical characteristics of SWCNT-based materials on their manufacturing and subsequent processing conditions, as well as on their partic-

ular properties including porosity, diameter of NT bundles, the degree of graphitization [6], chemical doping [7], and functionalization [8]. Thus, according to [6], the conductivity of films based on SWCNTs increases with the increasing degree of graphitization (the intensity ratio of the G and D modes (I_G/I_D) in the Raman spectra) and decreases with the increasing bundle diameter and porosity of the films. Doping of thin films containing pre-oxidized SWCNTs also results in a change in the conductivity. In this case both an increase in the conductivity as a result of doping (observed, particularly, in the case of doping with bromine [7] and thionyl chloride [8]) and a decrease in the conductivity (observed upon doping SWCNTs with aniline, PyPhF_5 , PhCH_2Br and others [9]) are possible. The ability to change the electronic properties of SWCNTs by doping, on the one hand, opens up the way for the development of nanoelectronic devices with desired electronic characteristics, and on the other hand, can serve as a basis for developing a new class of chemical sensors, electrical characteristics of which are sensitive to the presence of certain chemical compounds on the surface of NTs. All this calls for detailed studies aimed at determination of the dependence of the electrical characteristics of SWCNTs on their preparation conditions, temperature, and chemical environment, as well as the structural properties of a material containing NTs. In this paper, we present the results of measurements of the electrical resistance of SWCNT films depending on their preparation procedure and the structural features of these NTs over a wide temperature range.

Table 1. Methods of preparation and characteristics of the films studied in this work and published data: types of NTs, purification procedure, preparation conditions, size, ratio of peak intensities of Raman *G* and *D* bands (I_G/I_D), elemental composition according to the XPS data, measured resistance and calculated conductivity at room temperature

Sample, SWCNT type, purification procedure	Film preparation conditions	Dimensions of the film, $L \times W \times t$, μm	I_G/I_D	Elemental composition, wt %				R_{RT}, Ω	$\sigma_{RT} \times 10^3$, S/m
				C	O	Cl	Fe		
A, SM HiPCO SWCNTs	MVFS, toluene, drying in FV 360°C, 3 h	500 × 770 × 20	8.1	87.7	3.7	—	8.6	23.2	1.40
B, HiPCO SWCNTs, air/O ₂	MVFS, toluene, drying in FV 200°C, 6 h	1000 × 2070 × 40	4.8	91.4	5.1	1.7	1.8	2.4	5.03
C, Arc SWCNTs, air/O ₂	MVFS, toluene, drying in FV 450°C, 5 h	1140 × 2000 × 30	25	98.7	1.3	—	—	45	0.42
HiPCO SWCNTs (Purity >90%) [6]	MVFS, DMF, drying 20°C, 24 h	2200 × 20	15	—	—	—	—	—	16.7
Nanocyl SWCNTs (Purity >70%) [6]	MVFS, N-methylpyrrolidone, drying 20°C, 24 h	2200 × 20	11–14	—	—	—	—	—	2.08
Carbon Solutions Inc. SWCNTs-COOH (Purity 80–100%) [6]	MVFS, DMF, drying 20°C, 24 h	2200 × 20	3–10	—	—	—	—	—	13
SWCNTs (laser ablation of graphite), HNO ₃ [14]	—	1500 × 4000 × 200	—	—	—	—	—	10	0.2
HiPCO SWCNTs, air/O ₂ [9]	MVFS, SDS/H ₂ O, drying 100°C	—	—	—	—	—	—	—	55

EXPERIMENTAL

Two types of SWCNTs were used: ones obtained by chemical disproportionation of carbon monoxide on an iron catalyst at high pressure of CO and temperature (HiPCO SWCNTs with a diameter $d = 1.05 \pm 0.15$ nm, Carbon NanoTechnologies Inc.) [10], and others produced by thermal evaporation of graphite in the presence of a Ni–Y catalyst in an electric arc (Arc SWCNTs, diameter $d = 1.40 \pm 0.15$ nm) [11]. Films made of the source material (SM) and of purified NTs were studied.

The purification of SWCNTs was carried out by the oxidation of the material with oxygen, which included a stepwise oxidation in air flow by increasing the temperature by $\sim 50^\circ\text{C}$ at each stage in the temperature range 220–420°C. After each stage of the oxidation the material was treated with concentrated hydrochloric acid, filtered, rinsed with water, alcohol, and dried. At the last stage the material was annealed at $T = 800^\circ\text{C}$ for 1 h in a vacuum [12].

Films of SWCNTs (Backypaper) were formed by the method of vacuum microfiltration of suspensions (MVFS) of NTs in various solvents. The suspensions of NTs were prepared by dispersing the material with an initial concentration of 1 mg/ml in a solvent with ultrasound (UZDN-1, a frequency of 35 kHz, a power of 500 W) for 20 min upon thermostating the suspension at room temperature. The formation of the films was carried out by microfiltration of the suspension of SWCNTs in organic solvents through track membranes (nuclear filters, a thickness of 10 μm , a pore diameter of 0.2–0.4 μm , the material is polyethylene terephthalate). As a result of microfiltration, SWCNT

films of a necessary thickness were formed on the filter; they were repeatedly washed with solvents, dried in air and separated from the filter. The films then were further dried and annealed at different temperatures in forevacuum (a residual pressure of 10^{-4} mm Hg) for a few hours. The films were mechanically hard, flexible, opaque in visible light, and dark gray in color. The methods of preparation and characteristics of the films studied in this work (the types of NTs, conditions of preparation, size, intensity ratio of G and D modes (I_G/I_D) in the Raman spectra, elemental composition calculated from the XPS data, the experimentally measured resistance (R_{RT}, Ω) and the calculated conductivity ($\sigma_{RT}, \text{S}/\text{m}$) at room temperature are shown in Table 1. For comparison, Table 1 shows also published data for films obtained in a similar way. Films from the source material (SM) Arc SWCNTs containing ~ 15 –20 wt % NTs could not be obtained by this method.

The films were investigated by X-ray photoelectron spectroscopy (XPS) (MK II VG Scientific spectrometer, Al K_α photon energy 1486.6 eV), Raman spectroscopy (RS) (Nicolet NXR FT-Raman 9610 with an InGaAs detector, a semiconductor laser with an excitation wavelength of 976 nm and an output power of 1.2 W), and scanning electron microscopy (SEM) (Zeiss Leo Supra 25, accelerating voltage 2.88 kV, resolution 2 nm).

The temperature dependences of the resistivity $R(T)$ of the films of SWCNTs on the direct current were measured with the standard four-probe method using an automated setup for recording the resistance and temperature in the range 4.2–290 K [13]. A sam-

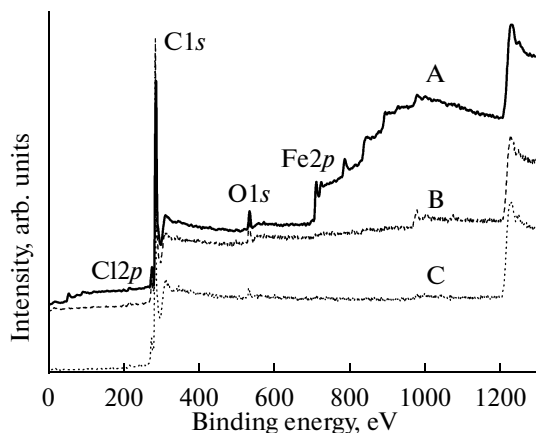


Fig. 1. The survey XPS spectra of the prepared films registered under excitation by photons with energy 1486.6 eV. Keys on the spectra correspond to the designations of the films in Table 1.

ple of the material was glued with a conductive graphite paste (Dotite paint, XC-12) to four platinum electrodes (10 μm diameter) of the measuring module. The temperature dependence of the resistance was measured in an inert atmosphere (He) in a storage helium Dewar vessel, the sample temperature was slowly varied from 290 to 4.2 K at a rate of ~ 1 K/min. The sample resistance was measured for two directions of current to eliminate the errors related to the thermo-EMF. The conductivity of the films was calculated by the formula $\sigma = L/RWt$, where L is the length, W is the width, t is the film thickness, and R is the experimentally measured value of the resistance of the film.

RESULTS AND DISCUSSION

The elemental composition of the films was determined by the XPS method. The survey photoelectron spectra of the films are shown in Fig. 1. The source material HiPCO SWCNTs (sample A) contains iron, which is a catalyst for the synthesis of NTs, and oxygen as impurities. The purification of HiPCO SWCNTs by oxidation with atmospheric oxygen drastically reduces the iron content and increases the oxygen content due to the oxidation of the surface of NTs (sample B). Traces of chlorine are present due to rinsing the material with hydrochloric acid to remove iron. The purification of Arc SWCNTs results in the oxidation of the surface of NTs (sample B) as well; as a result, the oxygen content reaches 1.3 wt %.

The morphology of the films, which is characterized by the porosity and average diameter of NT bundles, has been studied by scanning electron microscopy. The SEM images of the surface of the films based on Arc and HiPCO SWCNTs obtained by microfiltration of NT suspensions in toluene are shown in Fig. 2. As seen from Fig. 2, the films differ in morphology,

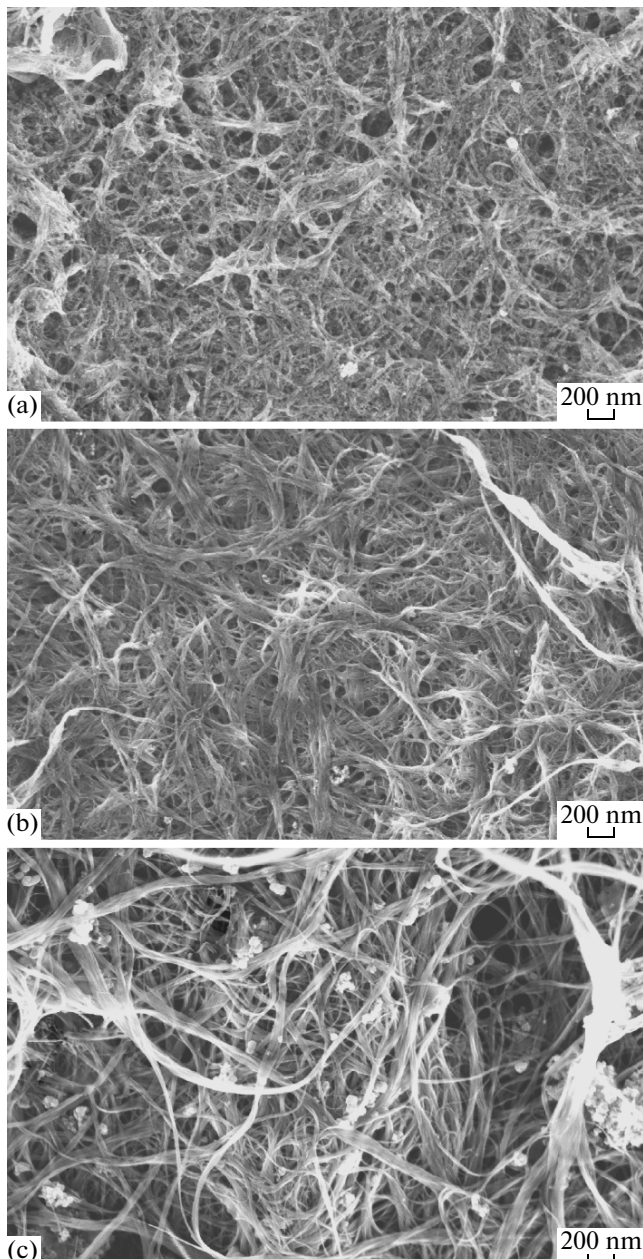


Fig. 2. SEM image of the surface of films based on HiPCO and Arc SWCNTs. Identifications of the films as in Table 1.

which is affected both by the type and purification of NTs. The film A from the HiPCO SWCNTs source material has uneven surface of randomly interwoven bundles of various sizes and contains visible admixtures of particles of metal catalyst, which are virtually absent in the films from purified NTs (B). The porosity of the films (P), i.e., percentage of free space (%) in a film was calculated by the following equation:

$$P = (1 - \rho_{\text{film}}/\rho_{\text{NT}}) \times 100\%, \quad (1)$$

where ρ_{film} is the density of the film, which was calculated on the basis of its mass and geometric dimensions, ρ_{NT} is true density of bundled NTs ($\sim 1.5 \text{ g/cm}^3$)

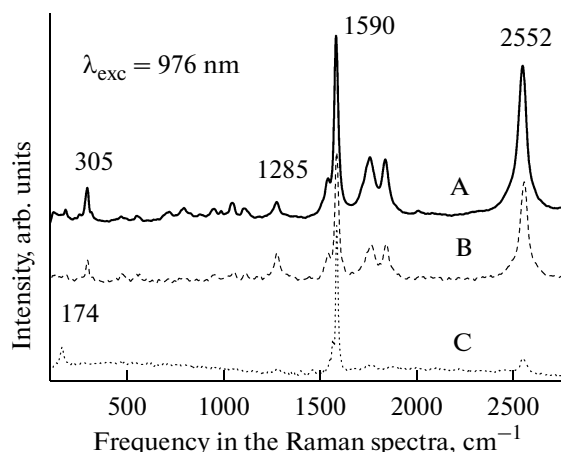


Fig. 3. Typical Raman spectra of films A, B (HiPCO SWCNTs), and C (Arc SWCNTs).

[15]. The values of porosity for films A, B, and C are 65, 72, and 76%, respectively. Films A and B have a lower porosity and a wide distribution of the average bundle diameters from 5 to 50 nm. Film C of Arc SWCNTs is more porous than A and B and has a greater average bundle diameter in a narrower size range of 20–40 nm.

The structural properties of SWCNTs were studied by Raman spectroscopy. Figure 3 shows the Raman spectra of the studied films (A, B and C), which include the radial breathing 305 cm^{-1} (A, B), 174 cm^{-1} (C) and tangential 1590 cm^{-1} (G band) modes, as well as D (1285 cm^{-1}) and D* (2552 cm^{-1}) bands. The intensity ratio of the peaks of G and D bands (I_G/I_D) in the Raman spectra, which characterize the degree of imperfection of the hexagonal structure of the surface of NTs or the degree of graphitization, are 8.1, 4.8, and 25 for A, B, and C, respectively. The comparison of the values of the I_G/I_D ratio for various film samples (Table 1) shows that in all cases the purification reduces this value. Similar results were obtained previously for HiPCO SWCNTs [16]. The imperfection of the graphite structure of the NTs and a decrease in the ratio of I_G/I_D upon the purification of NTs with the oxidizer O₂ is related to the opening of the ends of NTs, formation of vacancy defects, and functionalization of the surface of NTs with COOH– and OH– groups [17].

The results of the measurements of the resistance and conductivity of the HiPCO and Arc SWCNTs films (A, B and C) by the four-probe method at room temperature are shown in Table 1. These results are consistent with those of other authors for the films prepared by a similar method from different types of NTs [6, 9, 14]. Table 1 shows that films of purified NTs possess a higher conductivity. A low conductivity of the film C in comparison with A and B can be explained by an increase in its porosity and the average bundle diameter.

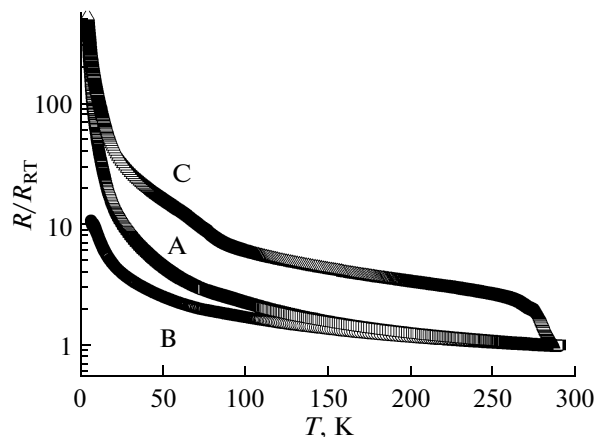


Fig. 4. The temperature dependence for the normalized resistance (R/R_{RT}) of the films on : A and B, HiPCO SWCNTs, and C, Arc SWCNTs.

Some conclusions on the conduction mechanism in SWCNTs films can be obtained by analyzing the temperature dependences of the resistivity of the films. These curves obtained in the temperature range 4.2–290 K for the films of different types are shown in Fig. 4. Figure 4 shows that the magnitude of the normalized resistance (R/R_{RT}) of the films decreases with the increasing temperature; with the decrements in the resistance upon the increase in temperature from 4.2 K (6.2 K) to room temperature being different for the HiPCO SWCNT films to make 360 (4.2 K) or 126 (6.2 K) for A and 11 (6.2 K) for B. For the Arc SWCNT films (C), the drop in R/R_{RT} from 4.2 K to room temperature is 523. The decrement in the R/R_{RT} value in the series of test HiPCO SWCNT films (A, B) in the examined temperature range decreases with increasing purity of the NT material used for making the films. The films consist of NTs with different electronic properties (from metallic to semiconducting ones with different band gaps); so, the temperature dependences of the conductivity are complex. Earlier [18], the dependence of the resistance of films on the ratio of metallic and semiconducting NTs in them was observed, and it was found [19] that the resistance of the films of the SM enriched with semiconducting NTs (> 90%) falls 10^4 times in this interval. It may be concluded that the higher values obtained in this work for the fall in R/R_{RT} of films A and B are due to the prevalence of semiconducting NTs in the film, and the decrease in the degree of the fall in R/R_{RT} values for purified films (B) is associated with changes in the ratio of metal and semiconducting NTs in the films during their purification. The dependence of the resistance of the films on their porosity, the bundle size, and functionalization of NTs was observed in [6, 20]. For example, it was shown [20] that the resistance of a bundle of individual NTs with a thickness of 35 nm is three orders of magnitude above that of the films based on the NTs. In this case, an approximately four-fold

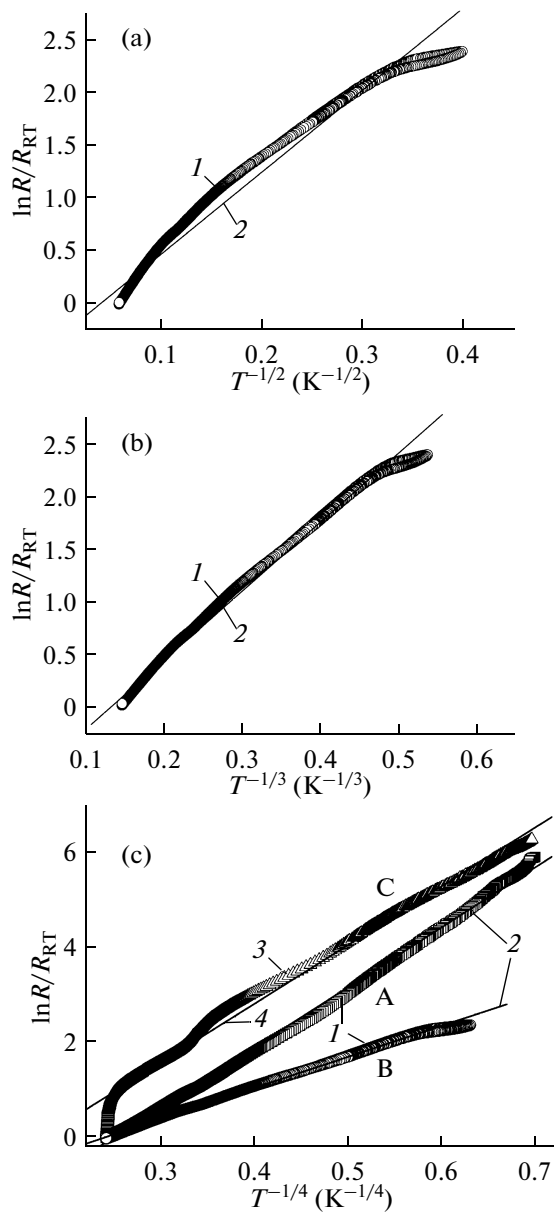


Fig. 5. Plots $\ln R/R_{RT} - T^{-1/(d+1)}$ for (a, b, c) HiPCO SWCNTs films B and (c) A; (c) for Arc SWCNTs films C based on the Mott hopping conductivity model: (a), $d = 1$; (b), $d = 2$; (c), $d = 3$; (a), (b), (c): 1, 3—experimental curves; 2, 4—dependences (1), (3) with the corresponding values of the dimension d .

drop in the resistance was observed in the same temperature range.

The descending mode of the temperature dependence of the resistivity indicates the semiconducting character of the conductivity of NT films. The conductivity of the samples at low temperatures is low, thereby indicating an insignificant contribution of metallic conduction. This seems natural, since only a third of NTs has a metallic conductivity, while the rest are semiconductors. Obviously, the conductivity of a complex structure containing a large number of

SWCNTs is determined by semiconducting NTs, which have a higher resistance at room and lower temperatures.

To describe the conductivity of disordered systems, to which the test SWCNTs films belong, two main mechanisms are used, the Mott hopping mechanism [21, 22] and the activation mechanism usually combined with the mechanism of tunneling conduction through metallic islets [9, 23]. In the hopping model, which is used to describe the conductivity of disordered semiconductor materials, the temperature dependence of resistance is determined by the following relationship:

$$R(T) = R_0 \exp\left[\left(\frac{T_0^{(d)}}{T}\right)^{1/(d+1)}\right], \quad (2)$$

where $T_0^{(d)}$ is a characteristic temperature, and d is the dimensionality of a conductor. According to Eq. (2), the temperature dependence of the resistance presented as a function $\ln R(T^{-1/(d+1)})$, should be a straight line, what can be used to determine the dimensionality d of a conductor. Figure 5 shows the corresponding plots for $d = 1$, $d = 2$, and $d = 3$ for HiPCO SWCNT film B, for which the coefficients of linear correlation are 0.9878, 0.9964, and 0.9987, respectively. Similar patterns were observed for films A and C (not shown), with linear correlation coefficients for HiPCO SWCNTs A ($d = 3$) and Arc SWCNTs C ($d = 3$) of 0.9990 and 0.9953, respectively. Thus, the experimental results are best described by Eq. (2) with $d = 3$ (Fig. 5).

This result indicates that electron transport in the materials is associated with three-dimensional hopping conductivity in semiconductors [14, 21, 24, 25]. Such a behavior can be explained by the defect structure of the films, in which electrons cannot restrict the movement only along the nanotube and jumps from one localized state to another or perhaps from one NT to another (from one bundle to another).

The above experimental dependences of the resistance on the temperature are approximated well by the following equation with $d = 3$:

$$\ln R/R_{290} = G + AT^{-1/4}, \quad (3)$$

where $A = (T_0^{(3)})^{1/4}$ is the constant of the Mott equation (2), and G is a quantity that depends on the geometric parameters of the film. Table 2 shows the values of the coefficients for the linear regression equation (3) and for comparison the value of the constant $A = 3.28$ for a film of SWCNTs prepared by laser ablation of graphite-based composite with a Fe : Ni catalyst [14]. A comparison of the coefficients G and A to the linear equation (3) (Table 2) for the test films shows that the higher the conductivity of the film, the lower the absolute value of G and A and the characteristic temperature.

Table 2. The coefficients for linear regression equation (3), characteristic temperatures, $g(\mu)a^3$ combinations (Eq. (4)), and conductivity at room temperature for the test films, and the data [14]

Film	G	A	$T_0^{(3)}$, K	$g(\mu)a^3 \times 10^{-4}$	$\sigma_{RT} \times 10^3$, S/m
A	-3.13	12.54	24728	8.6	1.40
B	-1.55	6.49	1774	119.5	5.03
C	-2.12	12.29	22814	9.3	0.42
[14]	-	3.28	116	1832	0.20

The values of the parameter A recovered on the basis of the treatment of the experimental data give information about the electronic properties of the disordered conductor consisting of SWCNT bundles. According to the percolation theory [22], this parameter is expressed in terms of energy density of electronic states of the conductor near the Fermi level $g(\mu)$ and the characteristic dimension a , on which the electron wave function of the localization center decreases:

$$A = \left[\frac{4N_c}{g(\mu)a^3} \right]^{1/4}. \quad (4)$$

Here, $N_c \approx 5.3$ is the dimensionless threshold concentration of localization centers, at which percolation first arises in the system of randomly located centers with energies randomly distributed in a certain range. Thus, the treatment of the experimental data obtained in this study allows us to determine the term $g(\mu)a^3$ (Table 2). The determination of each of these parameters separately requires another independent measurement, for example, the determination of the magnetoresistance of the sample [25].

The above conclusion on the three-dimensional nature of hopping conductivity in the SWCNT films is inconsistent with the assumption [25] on the two-dimensional character of the conductivity, although this assumption is likewise based on the results of treatment of the temperature dependences of the resistivity of SWCNT thin films.

However, comparing the results obtained in this study with the published data [25], an ~300-fold difference in the thickness of the films used here and in [25] should be taken into account. It seems that in a film with a thickness of ~100 nm [25], electron transitions between different bundles, whose transverse size ranges from several to several tens of nanometers, are less likely than the transitions between NTs belonging to a single bundle. This picture is consistent with the two-dimensional nature of hopping conduction. On the other hand, in films with a thickness of several tens of μm studied in this work the number of contacts between neighboring bundles is much larger, which explains the predominance of the three-dimensional hopping conduction mechanism in this case.

CONCLUSIONS

Films of SWCNTs have been prepared and characterized by Raman and X-ray photoelectron spectroscopy, scanning electron microscopy; their electrical resistance has been investigated in the temperature range of 4.2–290 K. The resistance of the films depends on the type and degree of purification of nanotubes and decreases with increasing temperature, the degree of incidence decreases with increasing purity of the nanotube material. The descending pattern of the temperature dependence of the resistivity shows the semiconducting character of conductivity in these films. This pattern of conductivity is the result of a combination of different types of dependences of the resistance of the films on the elemental composition, the ratio of metallic and semiconducting NTs, porosity, and the bundle size. The analysis of the temperature dependences of the resistivity of the films in terms of the Mott hopping conduction mechanism has shown that the electron transport in these films is consistent with the three-dimensional hopping conductivity.

ACKNOWLEDGMENTS

This work was supported by the Russian Foundation for Basic Research, project no. 08-03-01017.

REFERENCES

- Wu, Z., Chen, Z., Du, X., Logan, J.M., Sippel, J., Nikolou, M., Kamaras, K., Reynolds, J.R., Tanner, D.B., Hebard, A.F., and Rinzler, A.G., *Science*, 2004, vol. 305, p. 1273.
- Dillon, A.C., *Chem. Rev.*, 2010, vol. 110, p. 6856.
- Mahar, B., Laslau, C., Yip, R., and Sun, Y., *IEEE Sensors J.*, 2007, vol. 7, p. 266.
- Yang, W., Ratnac, K.R., Ringer, S.P., Thordarson, P., Gooding, J.J., and Braet, F., *Angew. Chem., Int. Ed. Engl.*, 2010, vol. 49, p. 2114.
- Eletskii, A.V., *Usp. Fiz. Nauk*, 2009, vol. 179, no. 3, p. 225.
- Lyons, P.E., De, S., Blighe, F., Nicolosi, V., Pereira, L.F.C., Ferreira, M.S., and Coleman, J.N., *J. Appl. Phys.*, 2008, vol. 104, p. 044302.

7. Fanchini, G., Unalan, H.E., and Chhowalla, M., *Appl. Phys. Lett.*, 2007, vol. 90, p. 092114.
8. Parekh, B., Fanchini, G., Eda, G., and Chhowalla, M., *Appl. Phys. Lett.*, 2007, vol. 90, p. 121913.
9. Skakalova, V., Kaiser, A.B., Dettlaff-Węglikowska, U., Hrnčáriková, K., and Roth, S., *J. Phys. Chem. B*, 2005, vol. 109, p. 7174.
10. Nikolaev, P., Bronikowski, M.J., Bradley, R.K., Rohmund, F., Colbert, D.T., Smith, K.A., and Smalley, R.E., *Chem. Phys. Lett.*, 1999, vol. 313, p. 91.
11. Lobach, A.S., Spitsyna, N.G., Obraztsova, E.D., and Terekhov, S.V., *Fiz. Tverd. Tela*, 2002, vol. 44, p. 457.
12. Blank, V.D., Ivdenko, V.A., Lobach, A.S., Mavrin, B.N., and Serebryanyaya, N.R., *Opt. Spektrosk.*, 2006, vol. 100, no. 2, p. 282.
13. Buravov, L.I., Zverev, V.N., Kazakova, A.V., Kushch, N.D., and Manakov, A.I., *Prib. Tekh. Eksp.*, 2008, vol. 51, no. 1, p. 169.
14. Hirahara, K., Suenaga, K., Bandow, S., Kato, H., Okazaki, T., Shinohara, H., and Iijima, S., *Phys. Rev. Lett.*, 2000, vol. 85, p. 5384.
15. Lyons, P.E., De, S., Blighe, F., Nicolosi, V., Pereira, L.F.C., Ferreira, M.S., and Coleman, J.N., *J. Appl. Phys.*, 2008, vol. 104, p. 044302.
16. Lafi, L., Cossement, D., and Chahine, R., *Carbon*, 2005, vol. 43, p. 1347.
17. Kukovecz, A., Kramberger, Ch., Holzinger, M., Kuzmany, H., Schalko, J., Mannsberger, M., and Hirsch, A., *J. Phys. Chem. B*, 2002, vol. 106, p. 6374.
18. Barnes, T.M., Blackburn, J.L., van de Lagemaat, J., Coutts, T.J., and Heben, M.J., *ACS Nano*, 2008, vol. 2, p. 1968.
19. Han, Z.J. and Ostrikov, K., *Appl. Phys. Lett.*, 2010, vol. 96, p. 233115.
20. Lee, R.S., Kim, H.J., Fischer, J.E., Lefebvre, J., Radosavljevic, M., Hone, J., and Johnson, A.T., *Phys. Rev. B*, 2000, vol. 61, p. 4526.
21. Mott, N.F. and Davis, G.A., *Electronic Processes in Noncrystalline Materials*, Oxford: Clarendon, 1979.
22. Shklovskii, B.I. and Efros, A.L., *Usp. Fiz. Nauk*, 1975, vol. 117, no. 3, p. 401.
23. Bekyarova, E., Itkis, M.E., Cabrera, N., Zhao, B.Yu.A., Gao, J., and Haddon, R.C., *J. Am. Chem. Soc.*, 2005, vol. 127, p. 5990.
24. Peng, H., *J. Am. Chem. Soc.*, 2008, vol. 130, p. 42.
25. Takano, T., Takenobu, T., and Iwasa, Y., *J. Phys. Soc. Jpn.*, 2008, vol. 77, p. 124709.